CHARECTERISATION TECHNIQUES

Abstract

Characterization techniques help in understanding the properties of materials at a fundamental level. This knowledge is critical in fields like materials science, where the properties of substances dictate their behavior and potential applications. Researchers use characterization techniques to study new materials, compounds, and structures, facilitating innovation and the development of new technologies, medicines, materials, and products.

Industries use characterization to optimize manufacturing processes, improve efficiency, and enhance the performance of materials in various applications. Characterization contributes to advancing scientific knowledge by unveiling the structures, properties, and behaviours of substances at various levels, leading to discoveries that deepen our understanding of the natural world.

In essence, scientific characterization techniques are indispensable tools that drive innovation, ensure quality, aid in problem-solving, and expand our understanding of materials and their applications across a wide range of scientific disciplines and industries.

This chapter emphasis on the detailed overview on Physio chemical properties study of materials in ten different sections. First section briefs about the need of characterization, second and third sections briefs about single crystal XRD and powder XRD studies respectively. chapter highlights the using X-ray diffractions. The fourth section focus on the Fourier transform infrared studies and in the fifth section discussion of UV Visible spectroscopy. The sixth section enlightens about the thermogravimetric analysis and

Authors

M R Hareeshkumar
Department of Physics
DVS College of Arts and Science
Constituent College of Kuvempu University
Shivamogga, Karnataka, India.
hari.melgiri@gmail.com

M R Jagadeesh
Department of Physics
Bapuji Institute of Technology
Affiliated to VTU Belagavi
Davangere, Karnataka, India.

followed by seventh section with FESEM and edax studies discussion. The dielectric studies and the micro hardness studies were discussed in the eighth and nine sections. Finally, the important tool to evaluate the nonlinear optical properties of the materials i.e., Kurtz powder method is discussed in detail in the last secttion.

Keywords: In essence, scientific characterization techniques are indispensable tools that drive innovation, ensure quality.

I. INTRODUCTION

In materials science, characterization denotes external methods to probe into a material's internal structure and properties. Actual materials testing or analysis may be used to characterize a material. Techniques are used to magnify the specimen, imagine its internal structure, and learn about the distribution of elements within the specimen and their interactions, for example, in certain study forms. A type of microscope is typically used for magnification and internal visualization.

The connection of physical and chemical properties with structural characteristics, manufacturing, and preparation conditions is crucial to creating novel products and enhancing prevailing products. A thorough understanding of a product's material properties under manufacturing or application conditions is essential for its performance. Another significant aspect of efficient product development and quality complications depends on macroscopic as well as microscopic material properties.

This chapter delivers an overview of the experimental techniques used to characterize the grown crystals in this study. Diffractometers are used to analyze the structure and crystalline nature. Fourier transform infrared (FTIR) spectroscopy identifies the different functional groups of the crystal. A TG-DTA thermal analyzer and UV-visible spectrometer were used to examine the thermal and linear optical properties.SEM and EDAX have been used to investigate the surface morphology and elements in the material. The frequency-dependent dielectric parameters were observed. Vicker's microhardness tester is utilized to assess microhardness and different mechanical parameters. Finally, The SHG efficiency of the grown crystals was detected by the Kurtz powder

II. CHARACTERIZATION AND EXPERIMENTAL TECHNIQUES

X – Ray Diffraction

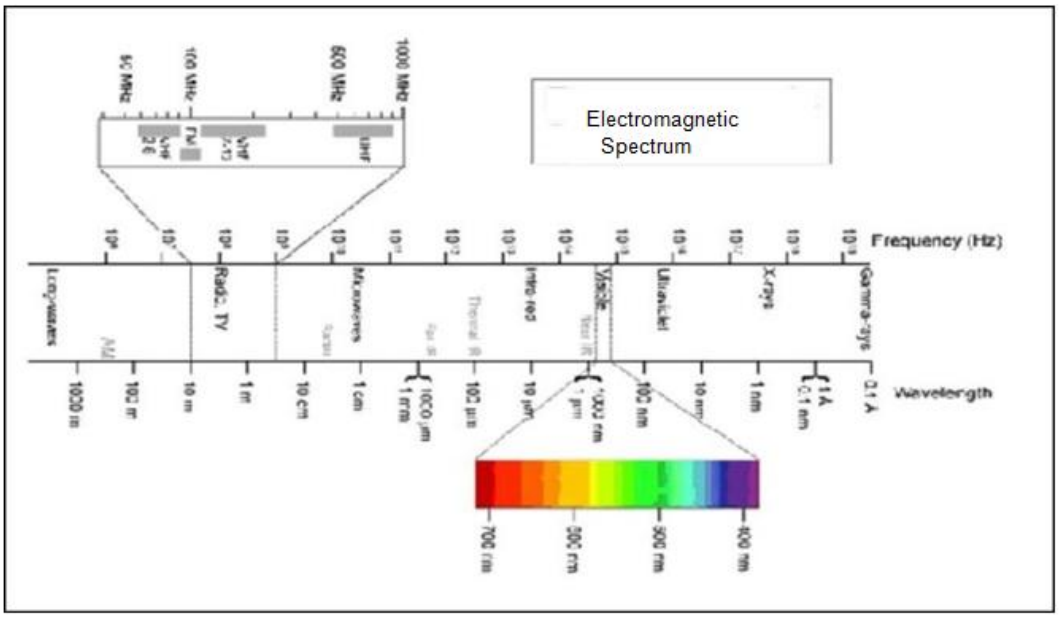

Figure 1: Electromagnetic Spectrum

X-ray diffraction is a non-destructive method for examining the structural aspects of crystalline solids, such as metals, electronic and geological materials, and organics. Figure 1 shows that the X-rays are part of the shorter wavelength of the electromagnetic spectrum (about $1A^0$). There are categories of X-ray diffraction methods: Single crystal and powder methods.

III. SINGLE CRYSTAL X-RAY DIFFRACTION ANALYSIS

This Characterization assists in determining the atomic positioning within the test sample. The several confines associated with molecular architecture is determined using this method. Figure 2 shows an instrument that comprises an X-ray production tube, a sample mounting space, and revealers.

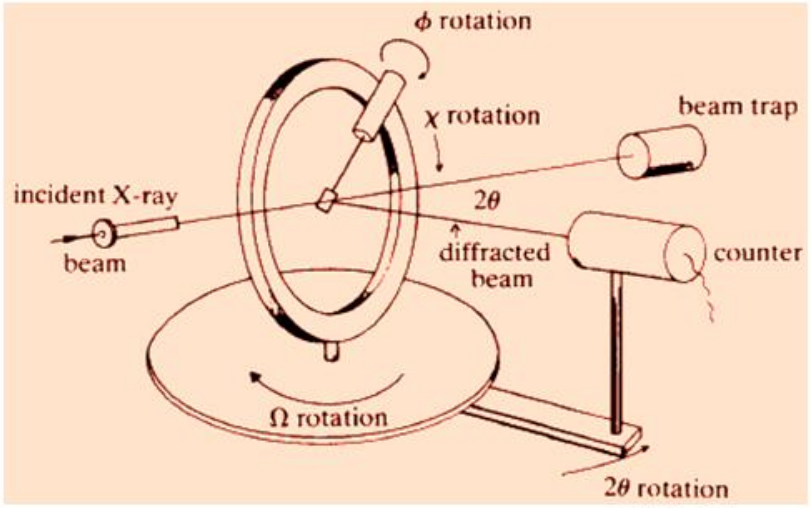

Figure 2: Geometry of Single-Crystal X-ray Diffractometer

A monochromatic fine X-ray beam are scattered on the sample so that the angle of planes of scattering satisfies Bragg's law well known equation which results, in constructive interference. Further, the detector collects scattered means diffracted X-rays of a specific orientation. Charge-coupled devices (CCD) convert X-ray photons into electrical signals in most modern single-crystal XRD diffractometer.

The sensor is attached to a device that keeps track of the signal's count rate. The present study determined crystal parameters using a Bruker Smart Apex Duo single-crystal X-ray diffractometer, shown in figure 3.Using the lattice parameters as well as space group, the single XRD analysis predicts the crystal systems and their symmetric conditions.

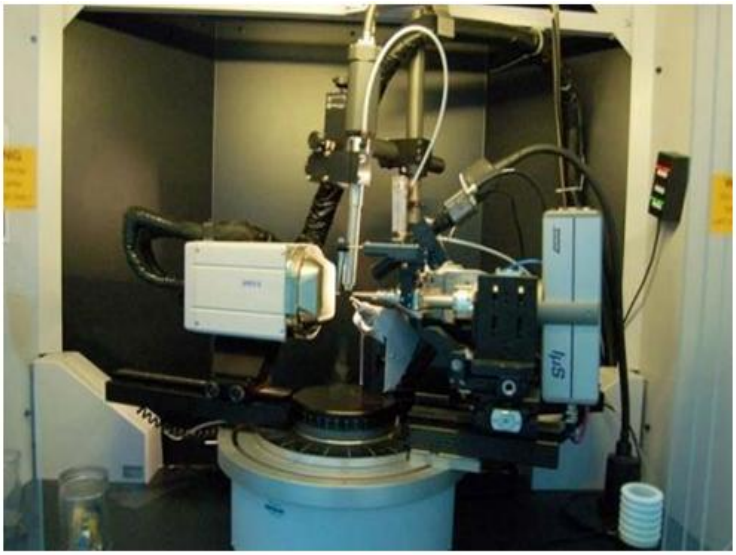

Figure 3: Bruker Smart Apex Duo Single Crystal X-Ray Diffractometer

1. **Powder X-Ray Diffraction Analysis:** Powder x-ray diffraction analysis helps understand the properties of all types of materials. X-rays beam is incident on a specimen and is dispersed X-ray by planes satisfying the Bragg's equation. The orientation of the crystal lattice concerning the incident beam determines the magnitude of diffracted light. Thus, the constructive interference circumstances are analogous to the law of reflection.

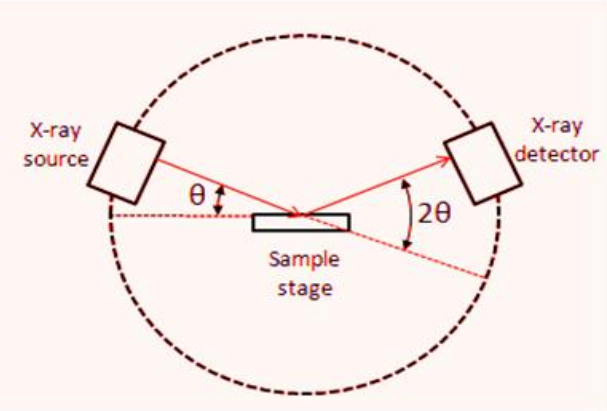

Figure 4: Schematic Diagram of a Powder X-ray Diffractometer

The instrument comprises of powdered content, goniometer and detector. The powdered sample provides possible orientations; the goniometer offers various incidence directions, and the sensor reads the strength of the resulting beam. Characteristically, the obtained results are graphed as a series of peaks with percentage intensity (on the Y-axis) and goniometer angle (on the X-axis). Here, the monochromator operate gives the detector a specific wavelength. Figure 4 graph will show which different phases are present in the study.

Figure 5 shows the X-ray study of the present work employing a Bruker AXS D8 progressive PXRD diffractometer with Cu-K radiations (=1.5406). The data was collected

inthe 2θ range at a 2^o per minute continuous scan speed.

Figure 5: Bruker AXS D8 Progressive PXRD Diffractometer

In XRD studies helps in finding the definite arrangement of atoms within the crystalline specimen for having definite peak. In general, the shift in the peak during the XRD analysis is due to linkage between host and doped particle, due to change in the size of the host particle and change in the binding energy and due to change in mechanical properties. Doping other atoms into a structure will lead to both peak shifts and changes in intensity.

The peak shifts occur because of the difference in size of the atoms, and cause the repeat distances in the crystal structure to expand or contract depending on whether the doped atom is larger or smaller than the host atom. The change in intensity occurs because the electron density of the doped atom is different than that of the surrounding atoms, and can make some peaks more intense and other peaks less intense. However, the degree of these changes depends on the concentration of the doping atom.

IV. FOURIER TRANSFORM INFRARED SPECTROSCOPY

It's a popular analytical method for determining the composition and structure of organic and inorganic substances. FTIR includes the target sample absorbing various infrared radiations and producing an IR spectrum that helps identify the substances. Figure 1.6 shows the spectral range of FTIR study for any crystal.

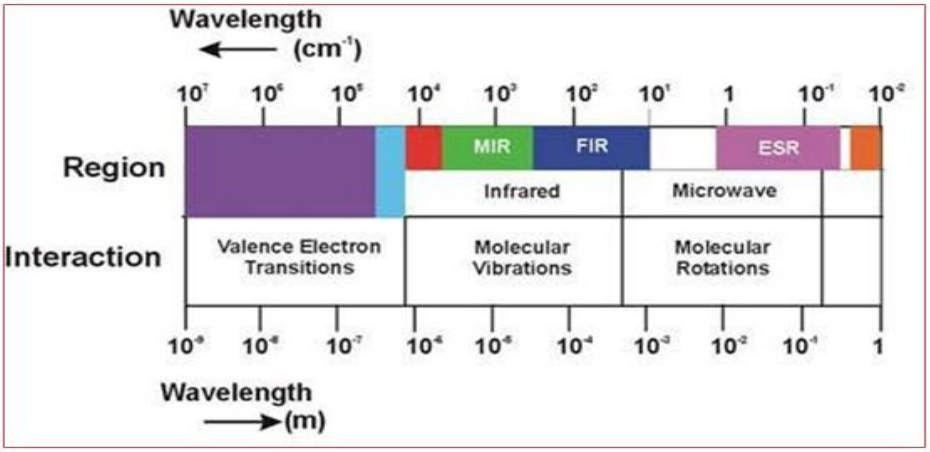

Figure 6: Spectral Ranges for FTIR study

Energy absorption occurs at resonance among the wavelengths of incident radiation and the molecule's vibrational frequency. Due to this, the molecules de-excite by releasing the absorbed energy, resulting in distinct IR peaks. Hence, the circumstances of the molecules in the testing sample are represented by these absorption bands. The infrared region is divided into three areas: near-infrared, mid-infrared, and far-infrared, and the functional groups attached to these regions are analyzed.

The characteristic wave number range of the near-infrared region is 12800-4000 cm^{-1}.Solid and liquid samples were analyzedusing diffusive reflectance or radiation absorption in this range. Wave numbers in the 4000- 200 cm^{-1} range are used in the mid-infrared studies. Composite gaseous, organic complexes, liquid or solid blends, pure solid or liquid samples, and atmospheric samples can all be studied using absorption, reflectance, or emission in this area.

Conversely, quantization of vibrational motion of molecules is taken into account. Hence, to excite a molecule from one vibrational frequency to another, it must be absorbed IR radiation of specific energy. Stretching and bending are the most basic vibrational movements in molecules caused by IR radiation.

These stretching modes may be symmetrical or asymmetrical. Bending vibrations includes scissoring, rocking, twisting, and wagging. Figure 1.7 depicts the various groups bending vibrations.

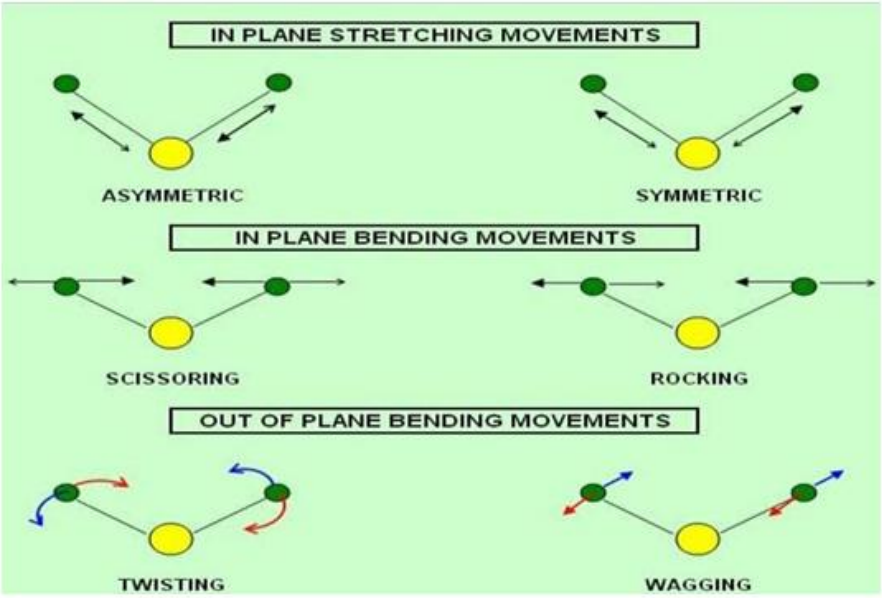

Figure 7: Vibrational Modes of Stretching and Bending in a Molecule

The inter-atomic range will shift continuously along the axis of the bond binding two atoms due to the stretching oscillations. In the case of organic crystals, FTIR assists in the identification of different functional groups as well as the confirmation of phase formation. The infrared spectrum region between 4000 and 1500 cm^{-1} is described as the functional group range. The peaks in this range represent the presence of functional groups in the molecule, while the region below 1500 cm^{-1} is known as the traits footprint region. Figure 8 signifies the distinctive Infrared region bands.

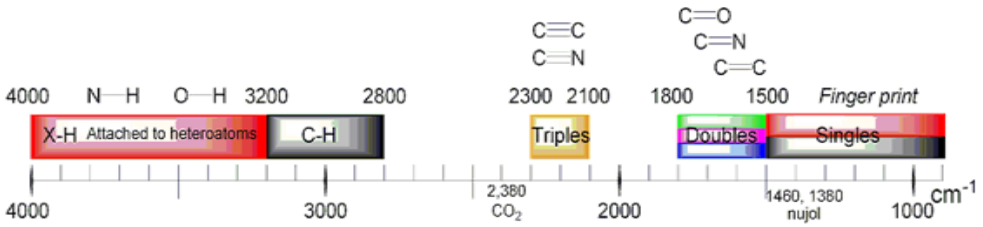

Figure 8: Graphical Depictions of IR Bands

Figure 9 shows the source, monochromator and detector that make up an IR spectrometer. The source is chosen to be stable and has an uninterrupted emission across the whole IR spectrum. Even though these radiations are continuous, the samples can only absorb particular frequencies. The Nernst glowers, which can reach 2200 K and a Glabor, which can reach 1500 K, are the most common sources. The strength of radiant energy depends on the source temperature. A bright energy source that allows for the isolation of narrow frequency bands is provided.

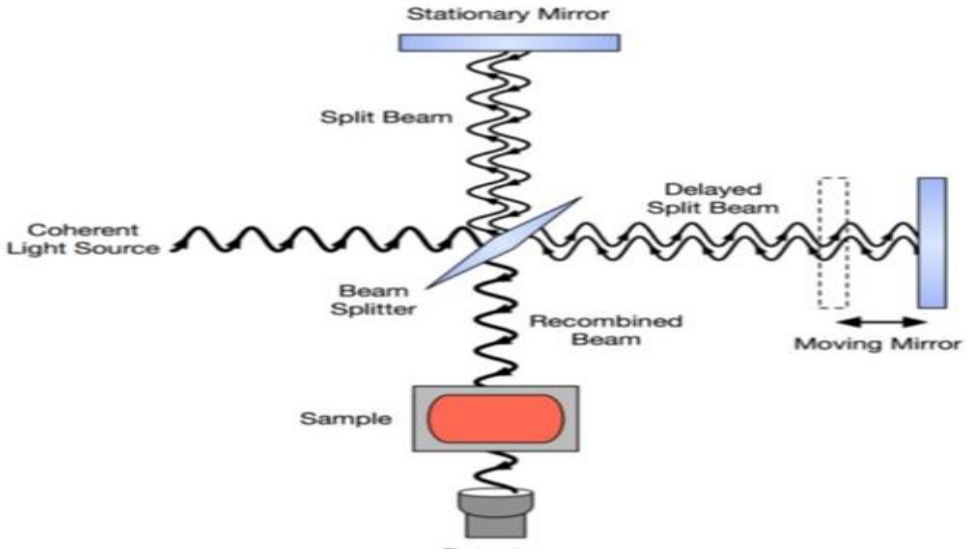

Figure 9: Typical FTIR Interferometer

The dispersive IR instruments consist of a monochromator(prism or diffraction grating)that absorbs the specific frequency of radiation. The detector is the set-up for the end part ofthe experiment to detect the radiations. The essential purpose of these infrared detectors is to calculate the source's IR energy and convert it radiation energy to electrical energy. Generally, IR region's radiant power is small, resulting in a low signal at the detector. A preamplifier is attached to the detector helps in amplifying the signals. The most widely used are Golay cells, Semiconductor detectors, and Pyroelectric detectors. FTIR spectrometers have a variety of benefits compared to dispersive IR spectrometers. Furthermore, the FTIR technique is utilized to examine gases, liquids, and solids in a short amount of time with minimal sample standardization. This analysis used a Bruker IFS FTIR spectrometer, as exposed in figure10.

Figure 10: Bruker IFS FTIR Spectrometer

V. ULTRAVIOLET-VISIBLE SPECTROSCOPY

UV-visible spectroscopy studies the optical absorption of a variety of materials quantitatively. The optical transparency of NLO crystals is one of the most significant

parameters for determining material capability for device fabrication. The UV region's energy is appropriate to cause electronic transitions and excitations at the levels of rotational, vibrational, and electronic energy called electronic spectroscopy. The electromagnetic spectrum's ultraviolet (UV) region ranges from 100-400 nm. Since the air molecules absorb radiation in this region, the vacuum UV (below 200nm) is only accessible with special vacuum equipment. There are three types of valence electrons in organic crystals that alter the electronic energy of the molecule by subsequent absorption of UV radiation, and they are

- **σ- Electrons:** These are electrons connected with saturated bonds, also known as σ bonds.

  Since the energy needed to excite electrons in σ bonds is substantially larger than that provided by UV light. bonds do not absorb UV light.
- **π- Electrons:** Unsaturated hydrocarbons, such as aromatic compositions, contain these electrons.
- **n- Electrons:** The bonding between the atoms in the particles is not affected by these electrons. UV radiation is absorbed by organic compounds containing nitrogen, oxygen,or halogen.

A transfer of valence electrons occurs as a complex molecule absorbs UV radiation. During these transitions, An electron moves up to the next higher orbital from an occupied orbital. The Probable modifications are $\sigma \rightarrow \sigma^*$, $n \rightarrow \sigma^*$, $n \rightarrow \pi^*$ and $\pi \rightarrow \pi^*$. Among these, $n \rightarrow \pi^*$modulation is forbidden when the selecting rule is employed. Figure 1.11 depicts a schematic representation of excitation energies.

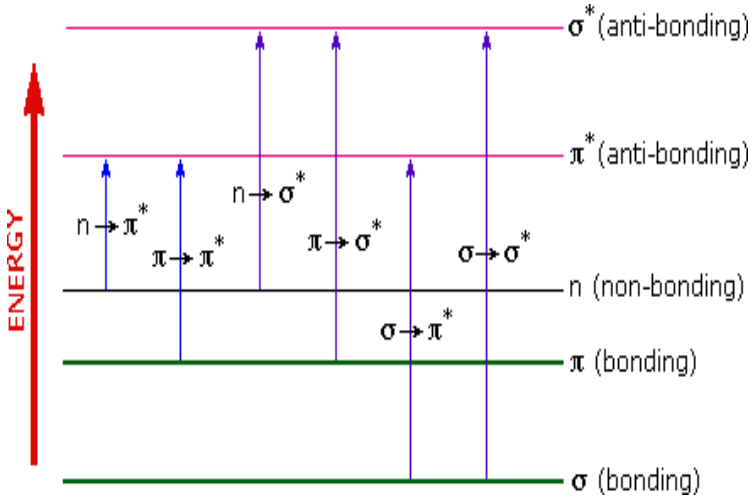

Figure 11: Electronic Excitation Energies

The UV-VIS spectrophotometer is extremely dependable, and its operation is relatively easy. The transmittance and absorbance can be calculated as,

$$\text{Transmittance} = \frac{I}{I_o}, \text{ and it is generally expressed in } \%T \qquad 1.1$$

$$\text{Absorbance } (\%) = -log\ (\frac{I}{I_o}) \times 100 \qquad 1.2$$

Where I is the intensities of incident light transients from the other side of the sample (I) by the initial intensity (I_O)

The absorption spectra result from electrons transition from a lower to a higher energy state, while UV emission spectra result from the reverse shift. The intensity of spectral lines is determined by the probability of electronic transitions occurring in the UV region. Single- beam or double-beam UV spectrophotometers are accessible. Light passes absolutely through the sample in the first case. By ignoring the test material, the preliminary strength

I_o is considered. Despite being the initial design, it is now widely utilized in educational and industrial labs. Figure 12 depicts its graphical presentation. The incident light will be splitin the second instance. One beam is called a sample beam and the other is called a reference beam since it passes through the sample. Figure 13 shows the ray diagram for this.

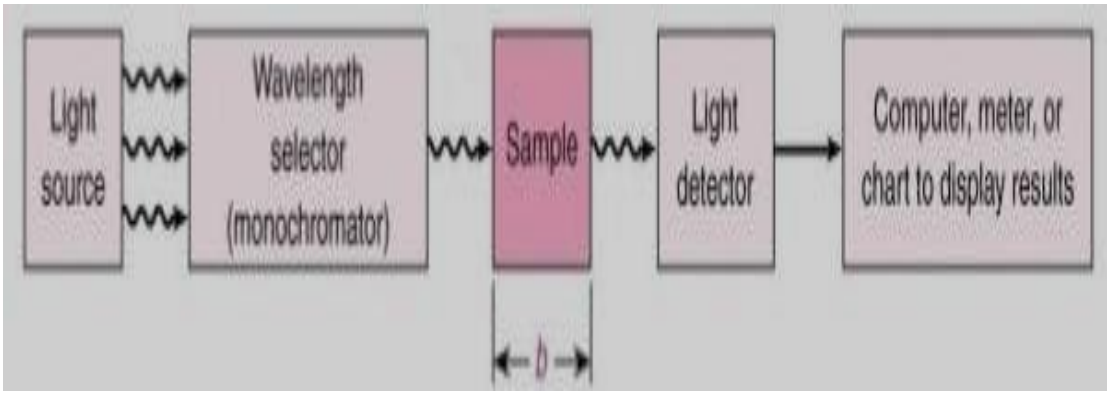

Figure 12: Configuration of a Single-Beam UV Spectrophotometer

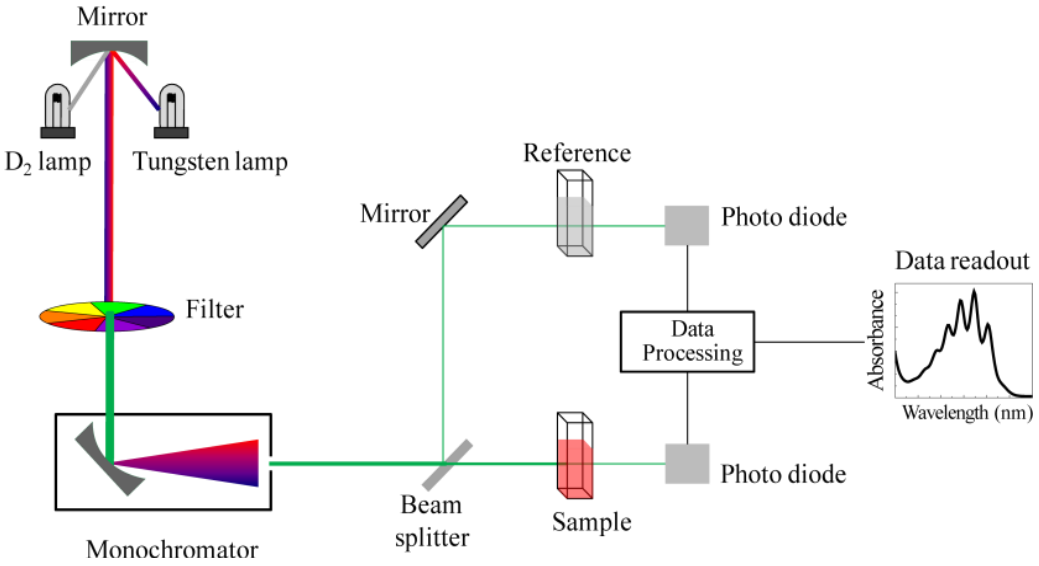

Figure 13: Configuration of a UV Spectrophotometer with Two Beams

The spectrophotometer uses a stable light source that can provide continuous radiation over the entire wavelength range. A tungsten lamp is used for visible light, and a deuterium or hydrogen lamp is used for UV light. A prism or plane grating separates a beam of light from each source into its component wavelengths. Glass, quartz, and fused silica are the most common materials used to make prisms.

The specimen absorbs a part of the incident beam while the remaining portion is conveyed to a detector. The monochromator's output radiation would be divided into two beams. The first incident is on reference, while the second fallson the specimen. The two rays are further focused on the detector. The detector's output is fed to an amplifier, which amplifies the transmitted light from both the sample as well as the reference.

The output waveform recorded on a meter, chart recorder or another form of readout system after being amplified. In terms of wavelength or frequency Vs transmission(T) or absorbance, the sample's spectrum thus represents a particular portion of the electromagnetic spectrum (A).

In the current research, UV experiments were conducted using a Varian Cary 5E spectrophotometer, depicted in figure 14.These spectral data were used to derive a number of optical properties, including the absorption co-efficient, optical reflectivity, refractive index and electrical susceptibility.

Figure 14: Varian Carry 5E Spectrophotometer

In general, the energy gap is calculated when the absorption of photons takes place. The optical band gap is a fundamental property of optical materials influenced by factors like crystalline nature and stoichiometry. In the present study, the absorption coefficient (α) was analyzed by articulating the absorbance by means of transmittance to calculate bandgap.

$$\alpha = \frac{1}{d} log \frac{1}{T} \qquad 1.3$$

Where, T is transmittance and D is thickness of the sample respectively.

Additionally, α estimates how much light can flow through the materials before being absorbed. It reflects the inter-band transition near the bandgap and is relative on both material properties and the wavelength of the light being absorbed. In the current work, for high photon energies (hν), the absorption coefficient was determined using the formula

$$\alpha h\nu = (h\nu - Eg) \qquad 1.4$$

Where Q is a transition relative parameter, h is Planck's constant, v is photon frequency,$E_g$is the material's bandgap and n is an index that can have any value(1/2, 1/3, 2, or 3) depending on the kind of transitions. The minimal-energy state in the conduction band and the maximal-energy state in the valence band are each characterized by a certain crystal momentum (k-vector) in the Brillouin zone. If the k-vectors are different, the material has an "indirect gap". a photon cannot be emitted because the electron must pass through an intermediate state and transfer momentum to the crystal lattice.

The band gap is called "direct" if the crystal momentum of electrons and holes is the same inboth the conduction band and the valence band; an electron can directly emit a photon. For the purposes of allowable direct transition, n is taken to be 1/2. Consequently, the equationis

$$\alpha = \frac{A(h\nu - Eg)^{1/2}}{h\nu} \qquad 1.5$$

By plotting the graph of $(\alpha h\nu)^2$ versus $h\nu$ in eV, for all of the grown crystals in this study, the bandgap value was calculated. Further, the resulting bandgap represents the visible region's transmittance.

Furthermore, the phrase destruction coefficient (K) relates to the nature of weak interaction or how intensely a material absorbs light at a specific wavelength. It can be calculated employing the equation.

$$K = \frac{\lambda\alpha}{4\pi} \qquad 1.6$$

As we know 'n' represents refractive index and also function of wavelength. The molar Extinction coefficient and refractive index are dependents on photon energy that designate the materials internal efficiency. Thus it is an essential crystal parameter to develop any solid- state electronic devices. The refractive index was analyzed through the formula [106].

$$\frac{n^4-1}{n^2+2} = 1 - \sqrt{\frac{E_g}{20}} \qquad 1.7$$

Where, E_g is the bandgap

The crystal optical reflectance was determined using the calculated refractive index valuesusing the equation below,

$$R = \frac{(n-1)^2}{(n+1)^2} \qquad 1.8$$

These linear optical variables can also be used to calculate the crystals' electrical susceptibility (χ_C), which is based on the fact that most naturally occurring compounds are non-magnetic at optical frequencies and hence, the refractive index is almost comparable to the relative permittivity of the material, and the analogous relationship is assigned by

$$\chi_c = \varepsilon_r - 1 \qquad 1.9$$

Or $\chi_c = n^2 - 1$

When the electrical susceptibility of a crystal is high (χ_c >1) it is easier to polarize the sample when intense light incidence it.

VI. THERMOGRAVIMETRIC ANALYSIS

Temperature dependent processing of samples is used to detect change in weight upon

temperature as well as time. The study of heat transfer across structures is frequently done using thermal analysis. In the present work, The Perkin Elmer STA 6000 thermal analyzer was used to calculate these parameters, as shown in figure 15.TGA records the precise weight of the sample as well as changes in temperature. GA is a common method for measuring material properties, moisture absorption by the sample, temperatures, decomposition points, and solvent residues, among other things. In DTA, a sample and an inert reference are heated or cooled as a function of temperature under identical conditions. As a result, measuring TGA and DTA simultaneously delivers heat flow and a rate of change in the weight of a sample in a controlled region as a function of temperature or time.

A thermo balance and a filled sample pan are usually found inside the furnace of a TGA analyzer. The null point weighing mechanism is used in the pan, usually platinum. The pan inside the furnace is electrically heated, and a thermocouple is used to measure the temperature precisely. A computer controls the unit's heating rate. The percentage sample weight (Y-axis) versus temperature (X-axis) will be plotted to test the sample. The testing of a specimen is carried with the gradual temperature rise. Transitions in DTA are caused by the sample emitting or absorbing energy compared to the reference and then plotted against time or temperature. This information can be used to determine whether the transformation is exothermic or endothermic. Changes in crystalline nature and dehydration reactions are described by sharp and large endothermic peaks, respectively. Chemical reactions in the oxidative environment, in particular, are primarily exothermic reaction.

Figure 15: STA 6000 thermal analyzer by Perkin Elmer

VII. FESEM AND EDAX STUDIES

The morphological investigation of the crystals can be aided by electron microscopy. Here, to obtain high-resolution images, the scanning is done using sample crossways. The generate the electron beam, the tungsten filament functions as a cathode in a vacuum in the SEM. The electrons emitted by the cathode attracted to the anode would be collimated as they pass through the condenser lens. Consequently, the objective lenses concentrate them on a specific point on the test sample. This is depicted schematically in figure 1.16. Finally, secondary electrons are generated when the electron beam comes into contact with the sample. A scintillation material that causes light flashes will be used to detect these.

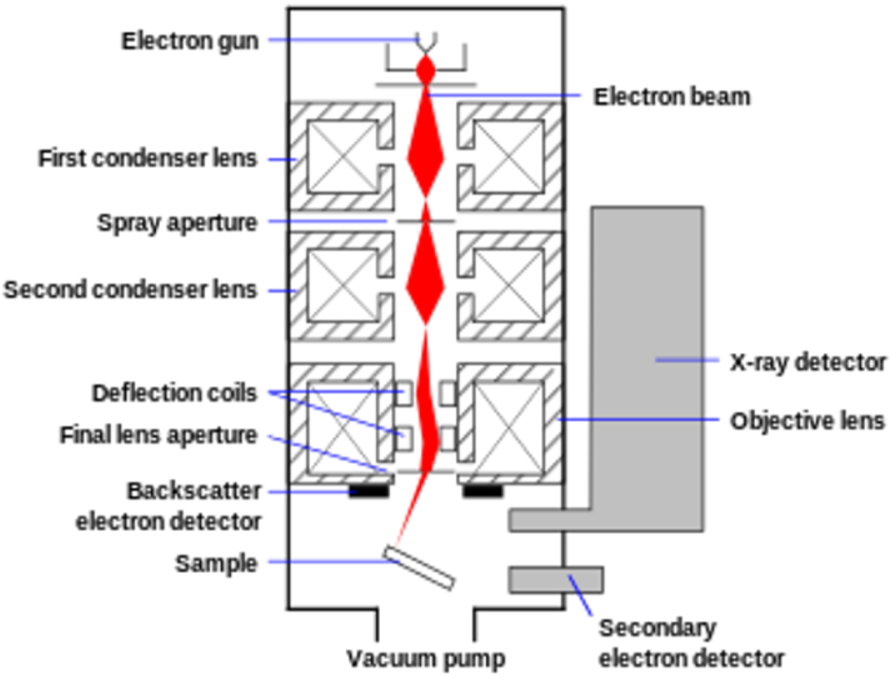

Figure 16: Schematic Representation of SEM-EDAX Analysis

The sample topography is specified in terms of light spots of varying intensities in the SEM image. The compositional information comes from the backscattered electrons. SEM includes the EDAX analysis system as a standard feature. During the EDAX investigation, the specimen electrons are bombarded with high-energy electrons, enabling them to transition to higher energy shells. X-rays are released as a result of these electrons' downward transition. The transformation releases a specific amount of energy, depending on the type of transition. The intensity V/S the energy of the released X–rays produce the EDAX spectrum. For the current study, the FEI QUANTA 200F and the JEOL Model JSM-6390 have used for SEM and EDAX study, as given in figure 17.

Figure 17: SEM-EDAXFEI QUANTA 200F and JEOL Model JSM-6390

VIII. DIELECTRIC STUDIES

The present research benefits in the interpretation of solids' electrical responses. As schematically depicted in figure 1.18, the dielectric constant and dielectric loss are both highly frequency dependent characteristics. The amount of electric stress and energy that is absorbed by the sample is referred to as the dielectric constant and loss in terms of the structure of atoms, ions, and bonding. The value of dielectric constant declines with expanding frequency in most organic and semi organic crystals, which is a typical dielectric activity.

Total polarization in a dielectric medium is determined by the dipoles' capacity to orient themselves in relation to the applied changing domain. At different frequencies, the frequency of polarization varies significantly. Electronic, ionic, dipolar and space charge polarizations are all feasible in the audio frequency range and the resultant polarizability is the sum of all of these. Due of the low frequencies involved. The dipoles would have enough time to align themselves with the field position. The dipoles would have enough time to align themselves with the field position. The dipole will easily obey the changing phrase if the relaxation time of the dipole is lower than half the length of the electric phrase. As the frequency rises, polarization mechanisms will be deactivated one by one as they are unable to react to the changing electric field. Electronic polarization makes an important contribution at higher frequencies (10^{15}Hz).

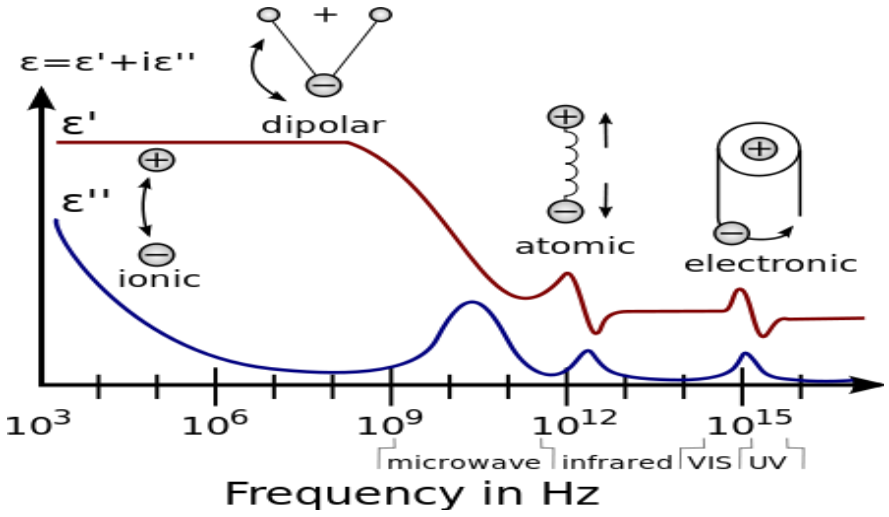

Figure 18: Dielectric constant frequency dependence in terms of different polarizations

Furthermore, the specimen is subjected to an electric phrase and over time turns into heat energy, a portion of the electrical energy is dissipated. In actual dielectric materials, this loss factor is regarded as a dielectric loss. A material must have a high-frequency region with little dielectric loss. This denotes a material's consistency, which dependent on the sample's purity and such samples have applications in the microelectronic industry.

Figure 19 represents the typical HIOKI 3532-50 HITESTER LCR meter utilized for determining dielectric parameters with variation in frequency range from100 Hz to 5 MHz at ambient temperature. To do this, silver paste was applied in layers to the sample's opposing

faces in order to produce an ohmic contact that might behave as a dielectric medium. The silver paste was carefully applied to the crystal's other sides to prevent it from spreading. The capacitance (C) and dielectric loss factor of the testing materials are determined by placing them between the copper platforms and electrodes.

The dielectric constant (ε_r)was evaluated using the formula

$$\varepsilon_r = \frac{Cd}{s_o A} \qquad 1.10$$

Where ε_o= 8.854×10^{-12} F/m is permittivity of the free space, $d$is thickness and A is the areaof the sample under investigation respectively.

$$tan\,\delta = {}^{1}/_{\omega cR} \qquad 1.11$$

Dielectrics only conduct a small amount of electric current in operation and they have resistivities between 1010 and 1020 ohm-m. The relationship between the dielectric constant and the dissipation factor was utilized to determine AC conductivity (ac).

$$\sigma_{ac} = \epsilon_r \epsilon_o \, 2\pi f \, tan\delta \qquad 1.12$$

This limitation helps in determining the impact of space charge polarization on crystal growth.

Figure 19: HIOKI 352-50 LCR HITESTER

IX. MICRO HARDNESS STUDIES

The microhardness analysis aids in the apprehension of the sample strength and deformation. It's also worth noting that the mechanical features of NLO specimen are highly correlated. The resistance to composition destruction or deformation is measured by hardness. Its value is evaluated by the elasticity and plasticity of the indenter material under evaluation, as well as the quantification conditions. The three hardness measurements are Scratch stiffness, indentation stiffness and dynamic stiffness. The indentation hardness measure is ideally fitted for samples divided into micro and macro indentation. The forces in

a micro indentation test usually are less than 2N. Figure 1.20 shows that pre-polished surfaces involve testing materials with low applied loads.

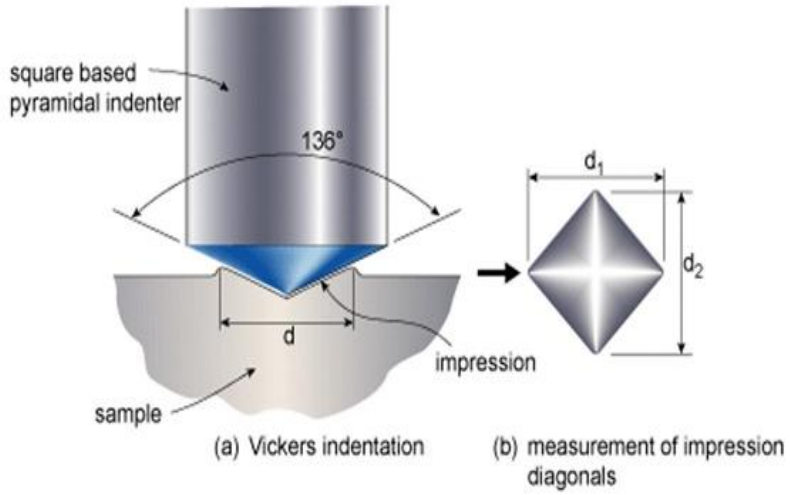

Figure 20: A typical Vickers's Diamond Pyramid Indentor

Using a source-based pyramid indenter, Vickers static micro indentation measurements were performed. The experiments are carried out at room temperature. The most widely accepted pyramid indenter is one whose opposite sides intersect at the apex at an angle (α) of 136°.The proportion of the applied load to the indentation region is known as hardness. Hence, the Vicker's hardness number H_V is expressed as

$$H_V = \frac{Load}{Pyramidal\,area} = \frac{2Psin(\alpha/2)}{d^2} = \frac{1.8544\ P}{d^2}\ \text{Kg/mm}^2 \qquad 1.13$$

Where, 'P' is applied weight in gm and 'd' is the average diagonal length in micrometer. Different weights ranging from 5 to 250 gms may be used for indentation. The size of the indentation impression is measured using a calibrated microscope. According to Mayer's rule, the relationship between applied weight and indentation size is given by

$P = kd^n$ or

$$\log p = \log k + n \log d \qquad 1.14$$

Where, k is constant for a particular sample. The value of 'n' refers to Mayer's index. Plotting the usually linear graph of log p and log d yields the value of n and the consequent slope is calculated. If n>2, H_V will increase with weight and $H_V$will lower if n <2.

Furthermore, for hard samples, the value 'n' should be between 1 and 1.6, while for soft materials, it should be greater than 1.6.The grown crystals were classified based on this information. The hardness study helps in understanding the strength and deformation of the crystal.

Hardness is a measure of resistance against structural destruction or deformation. Its

value depends on elastic and plastic properties of indenter material under test and also measurement conditions. Micro indentation test is usually has forces less than 2N. It involves testing of materials with low applied loads and pre polished surfaces, for using this indentation test to find out liquid inclusions.

The elastic stiffness constant (C11) is a material quality that indicates how much energy can be absorbed by the material before it fractures. It also measures resistance to deformation by a load applied to the flat crystal surface. The tightness of the bonding with neighboring atoms and the rate of variance with atom position are the two most significant factors in determining C11 values.

The corresponding C 11 value for the applied weights on the sample was calculated using the formula below. The Wooster formula

$$C_{11} = (Hv)^{\frac{7}{4}} \qquad 1.15$$

Yield strength (σ_V) is the stress under which a specimen begins to warp plastically beforedeforming elastically. The value of $\sigma_V$was evaluated by using the formula

$$\sigma_V = \frac{H_V}{2.9}[1-(n-2)]\left(\frac{12.5(n-2)}{1-(n-2)}\right)^{n-2} \qquad 1.16$$

The mechanical parameters of the current study were measured using a SHIMADZU HMV- 2T microhardness tester, as shown in figure 21 and in the relevant chapters, the estimated mechanical parameters are tabulated.

Figure 21: SHIMADZU HMV-2T Microhardness Tester

X. TECHNIQUE OF KURTZ POWDER FOR DETERMINING NLOPROPERTIES

It is among the most popular technique for determining the properties of NLOs. Crystallographers use this approach to determine if the structure's center of symmetry is absent. This method helps determine the impact of grain size on conversion efficiency and compares effectiveness to available material. In addition, It is possible to evaluate the noncritical phase-matching wavelength for a particular material and the capability to phase match using a tunable laser.

A beam of laser is used to incident a solid microcrystalline material in the Kurtz technique. The second harmonic wave is captured, filtered, identified and compared to a standard. Since the response's magnitude depends on particle size, caution should be exercised when preparing the crystal (e.g. Using a sieve to ensure a limited range of particle sizes). Figure 22 depicts the experimental diagrammatic configuration of a slightly changed Kurtz Perry setup.

The reference and excitation sources were both a Nd: YAG pulsed laser. The beam was split into two parts, one for reference and other for excitation. A photomultiplier was also used to detect the reference beam and determine its beam energy. The second will be used to elicit a response from the test sample. To obtain SHG intensity, the output light intensity was recorded on an oscilloscope. The elementary and harmonic intensitiesratio determines the sample's efficiency. Additionally, a sample of urea or KDP with equivalent particle size to be measured and an efficiency ratio will be depicted, to prevent potential experimental set-up errors. Figure 23 depicts the powder SHG quantification experimental setup.

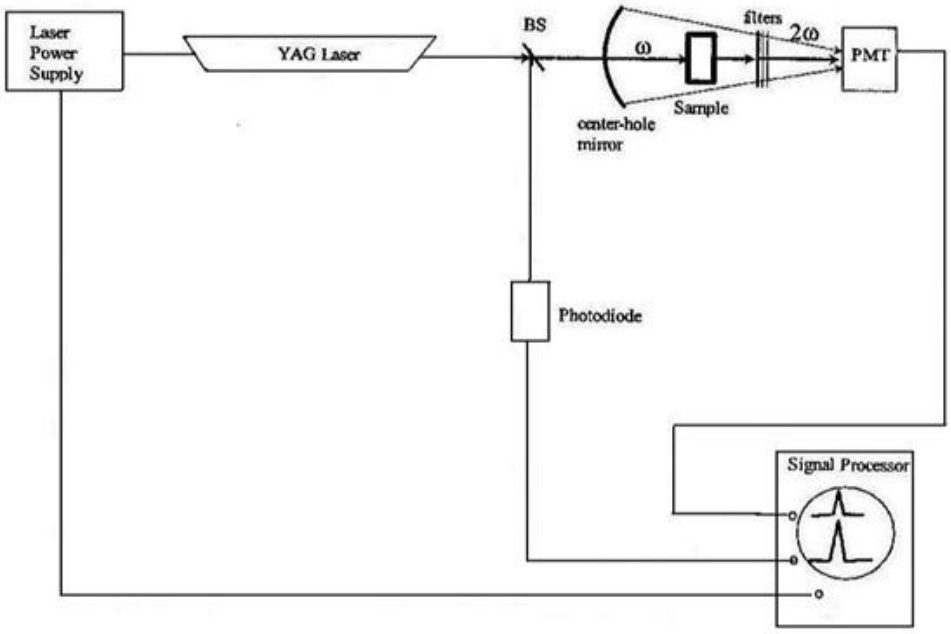

Figure 22: Schematic Design of Kurtz Powder Method

Figure 23: Experimental Set Up of Powder NLO Test

